Desalination and Water Treatment
www.deswater.com

doi: 10.1080/19443994.2015.1119759

57 (2016) 21476–21486
September

Taylor & Francis
Taylor & Francis Group

Analysis of phosphate removal from aqueous solutions by hydrocalumite

Jeong-Woo Son[a], Jae-Hyun Kim[a], Jin-Kyu Kang[a], Song-Bae Kim[a,b,*], Jeong-Ann Park[c], Chang-Gu Lee[c], Jae-Woo Choi[c], Sang-Hyup Lee[c,d]

[a]*Environmental Functional Materials & Water Treatment Laboratory, Seoul National University, Seoul 151-921, Korea, Tel. +82 2 880 4595; emails: sjw3520@snu.ac.kr (J.-W. Son), kjh85@snu.ac.kr (J.-H. Kim), naengie@snu.ac.kr (J.-K. Kang), Tel. +82 2 880 4587; email: songbkim@snu.ac.kr (S.-B. Kim)*

[b]*Department of Rural Systems Engineering and Research Institute of Agriculture and Life Sciences, Seoul National University, Seoul 151-921, Korea*

[c]*Center for Water Resource Cycle Research, Korea Institute of Science and Technology, Seoul 136-791, Korea, Tel. +82 2 958 5822; emails: d15506@kist.re.kr (J.-A. Park), changgu@kist.re.kr (C.-G. Lee), plead36@kist.re.kr (J.-W. Choi), yisanghyup@kist.re.kr (S.-H. Lee)*

[d]*Graduate School of Convergence Green Technology & Policy, Korea University, Seoul 136-701, Korea*

Received 10 August 2015; Accepted 24 October 2015

ABSTRACT

In this study, phosphate (P) removal from aqueous solutions by hydrocalumite was investigated using batch experiments and model analyses. The maximum phosphate removal capacity was determined to be 127.53 mg P/g under the given experimental conditions (hydrocalumite dose = 0.05 g/L, initial P concentration = 2–20 mg P/L, reaction time = 24 h). Model analyses showed that the Elovich model was most suitable for describing the kinetic data, whereas the Redlich–Peterson model provided the best fits to the equilibrium data. Furthermore, phosphate removal by hydrocalumite was not sensitive to pH changes between 4.0 and 11.0. A thermodynamic analysis indicated that phosphate removal by hydrocalumite increased with a rise in temperature from 15 to 45°C, suggesting that the removal process was spontaneous and endothermic (ΔH° = 32.05 kJ/mol, ΔS° = 112.86 J/K/mol, ΔG° = −0.47 to −3.86 kJ/mol). The phosphate removal capacity in stream water (5.40–17.25 mg P/g) was also lower than that in a synthetic P solution (6.86–27.51 mg P/g) under the given experimental conditions (initial P concentration = 2 mg P/L, hydrocalumite dose = 0.05–0.3 g/L, reaction time = 24 h). Such a result could possibly be ascribed to the presence of carbonate ions (CO_3^{2-}) in the stream water, which could interfere with phosphate removal by hydrocalumite through the precipitation of calcium carbonate ($CaCO_3$).

Keywords: Hydrocalumite; Hydroxyapatite; Layered double hydroxide; Phosphate removal; Precipitation

1. Introduction

Hydrocalumite is an anionic clay mineral with portlandite-like principal layers in which one-third of the Ca^{2+} sites are substituted by Al^{3+} ions [1]; it has the chemical formula, $Ca_4Al_2(OH)_{12}Cl_2{\cdot}4H_2O$, which is the Friedel phase [2]. Since hydrocalumite is mainly found in hydrated cement paste, it can be synthesized in a simple and inexpensive manner via hydration

*Corresponding author.

1944-3994/1944-3986 © 2015 Balaban Desalination Publications. All rights reserved.

reactions [3]. As layered double hydroxides (LDHs) [4], hydrocalumite belongs to a class of nanostructured anionic clays consisting of positively charged brucite-like sheets that are balanced by the intercalation of anions in the hydrated interlayer regions. LDHs have the general formula $[M^{2+}_{1-x}M^{3+}_{x}(OH)_2]^{x+}(A^{n-})_{x/n}\cdot mH_2O$, where M^{2+} is a divalent cation, M^{3+} is a trivalent cation, x is the molar ratio of $M^{3+}/(M^{2+} + M^{3+})$, and A is an interlayer anion with valence n [5]. These materials have a high surface area, large anion exchange capacity, and good thermal properties [6]. Recently, LDHs have been widely applied for the removal of contaminants from aqueous solutions [7–11].

Phosphate is an essential macronutrient in aquatic environments. However, the presence of phosphate in excessive amounts causes eutrophication in water bodies, which in turn leads to algal bloom in rivers, lakes, reservoirs, and coastal waters [12]. Various treatment methods (e.g. chemical, biological, and membrane technologies) have been employed to mitigate the phosphorus concentration in wastewater before its discharge into water bodies [13]. Recently, hydrocalumite has been used by several researchers for phosphate removal [14]. Oladoja et al. [2] synthesized hydrocalumite from a gastropod shell so as to examine its ability to remove phosphate from aqueous solutions. A research group from Shanghai University [4,15–18] also prepared hydrocalumite for the removal of phosphate from aqueous solutions. The authors subsequently characterized phosphate removal by hydrocalumite using batch removal experiments. Most of the research cited above was performed with high phosphate concentration ranges (25–326 mg P/L), the exception being the Ashekuzzaman and Jiang study [14], where experiments were conducted with a phosphate concentration of 10 mg P/L. It was reported that the phosphate concentrations in secondary effluents from municipal wastewater treatment plants were < 8.0 mg P/L [19,20]. At present, further experiments are required to clearly elucidate the performance of hydrocalumite in phosphate removal at low phosphate concentrations.

The aim of this study was to examine the removal of phosphate from aqueous solutions by hydrocalumite. Batch experiments were performed to investigate the effects of the reaction time, initial phosphate concentration, initial solution pH, temperature, and hydrocalumite dose on the removal of phosphate by hydrocalumite. Additional batch experiments were conducted in order to compare the phosphate removal performance in a synthetic phosphate solution and real stream water. Kinetic, equilibrium isotherm, and thermodynamic models were used to analyze the batch experimental data.

2. Materials and methods

2.1. Synthesis and characterization of hydrocalumite

All chemicals utilized for the experiments were purchased from Sigma Aldrich. Hydrocalumite (Ca_2Al-Cl LDH) was prepared in powder form by a co-precipitation method [16] using mixtures of calcium chloride ($CaCl_2$) and aluminum chloride hexahydrate ($AlCl_3{\cdot}6H_2O$). A 200 mL solution (Ca:Al molar ratio = 2) of $CaCl_2$ and $AlCl_3{\cdot}6H_2O$ was added dropwise to a 400 mL alkali solution (pH 13) of sodium hydroxide (NaOH) using a peristaltic pump (QG400, Fasco, Springfield, MO, USA). The dropwise addition was performed under an N_2 flow at a rate of 3 mL/min with vigorous stirring at room temperature. The resulting precipitates were aged at room temperature for 24 h in the mother liquor. Precipitates were then washed thoroughly with deionized water so as to remove excess sodium, and the final suspensions were centrifuged at 11,200× g (8,500 rpm) for 20 min. The washed precipitates were thermally treated at 105°C for 12 h in an electric muffle furnace (C-FMA, Vision Lab, Seoul, Korea), and subsequently pulverized in a ball mill [21].

Hydrocalumite was examined using a field emission scanning electron microscope (Supra 55VP; Carl Zeiss, Oberkochen, Germany). As evident from the FESEM image in Fig. 1(a), powder-type hydrocalumite was successfully synthesized. Energy dispersive X-ray spectroscopy (EDS) analysis was performed using the FESEM system, and the presence of calcium (Ca) with L-alpha and K-alpha peaks at 0.341 and 3.691 keV, respectively, was confirmed. Aluminum (Al) was also present with K-alpha and K-beta signals at 1.486 and 1.553 keV, respectively. The EDS examination indicated that the weight percents of Ca, Al, and Cl in the hydrocalumite (Ca_2Al-Cl LDH) were 28.50, 11.65, and 10.51%, respectively. Nitrogen gas (N_2) adsorption–desorption experiments were conducted with an ASAP 2020 instrument (Micromeritics, Nocross, GA, USA). The hydrocalumite particles had a specific surface area of 7.50 m^2/g, a total pore volume of 0.032 cm^3/g, and an average pore diameter of 16.89 nm. To characterize the hydrocalumite structure before and after the phosphate removal experiments, powder X-ray diffractometry (XRD, D8 Advance, Bruker, Germany) was performed with Cu Kα radiation (λ = 1.5406 Å) at a scanning speed of 0.6°/s.

2.2. Phosphate removal experiments

The desired phosphate (P) solution was prepared by diluting a stock solution (1,000 mg P/L) made from

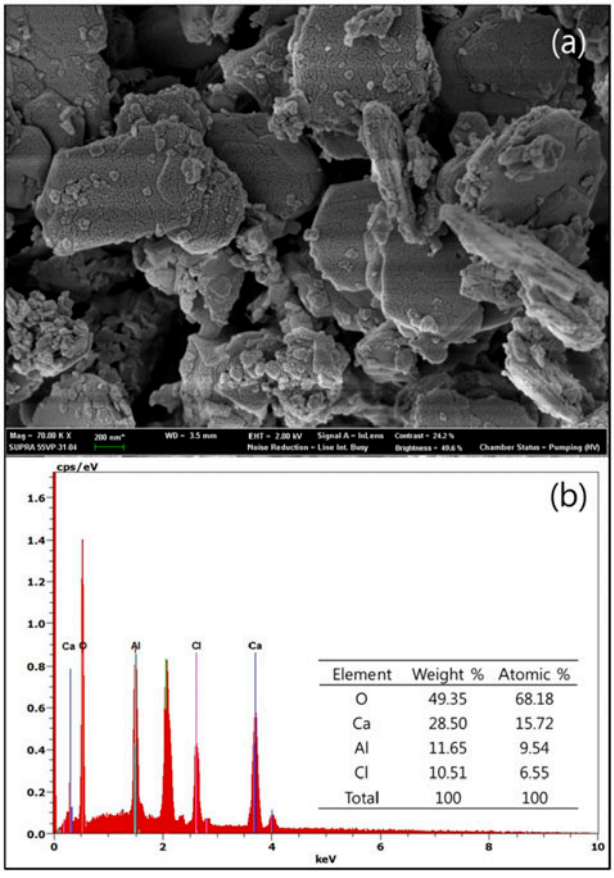

Fig. 1. Characteristics of hydrocalumite: (a) FESEM image (scale bar = 200 nm) and (b) EDS pattern (inset: elemental composition of hydrocalumite).

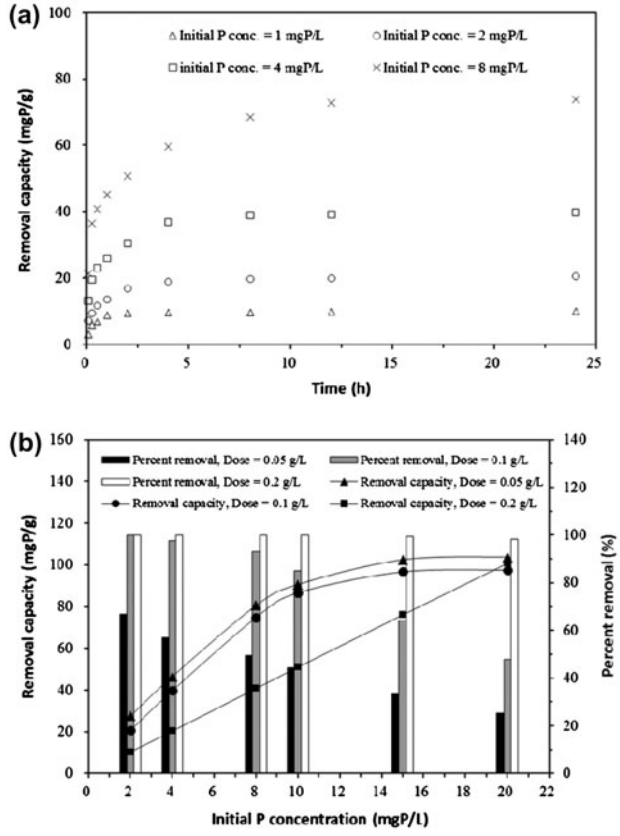

Fig. 2. Phosphate removal by hydrocalumite: (a) effect of reaction time and (b) effect of initial phosphate concentration.

potassium dichromate (KH_2PO_4). To investigate phosphate removal by hydrocalumite, batch experiments were performed at 30°C using 50 mL polypropylene conical tubes, unless otherwise stated; all experiments were carried out in triplicate. The first set of experiments was conducted to observe the effect of the reaction time on phosphate removal by hydrocalumite. The tests were performed at initial P concentrations of 1, 2, 4, and 8 mg P/L with a hydrocalumite dose of 0.1 g/L in 30 mL of solution. The tubes were shaken at 100 rpm using a shaking incubator (Daihan Science, Seoul, Korea), and samples were collected after various reaction times. Collected samples were subsequently filtered through a 0.45 μm membrane filter. The phosphate concentration was measured by the ascorbic acid method [22] at a wavelength of 880 nm using a UV–vis spectrophotometer (Genesys 10S, Thermo Scientific, Waltham, MA, USA).

The second set of experiments was performed to investigate the effect of the initial phosphate concentration on the phosphate removal performance. Hydrocalumite (dose = 0.05, 0.1, 0.2 g/L) was added to 30 mL of a phosphate solution (initial concentration = 2–20 mg P/L), and samples were collected after 24 h. The third set of experiments was conducted to examine the effect of the initial solution pH (initial P concentration = 2 mg P/L, hydrocalumite dose = 0.1 g/L, reaction time = 24 h). Here, 0.1 M NaOH and 0.1 M HCl solutions were utilized to adjust the pH of the reaction solution from 4.0 to 11.0; the pH was measured with a pH probe (9107BN, Thermo Scientific, Waltham, MA, USA). The fourth set of experiments was performed at 15, 30, and 45°C in order to elucidate the effect of temperature on phosphate removal (initial P concentration = 2 mg P/L, hydrocalumite dose = 0.05 g/L, reaction time = 24 h).

The fifth set of experiments was performed to evaluate the effect of the hydrocalumite dosage on phosphate removal (initial P concentration = 1–8 mg P/L, hydrocalumite dose = 0.05–0.3 g/L, reaction time = 24 h). Additional tests were conducted with stream water (initial P concentration = 2 mg P/L, hydrocalumite dose = 0.05–0.3 g/L,

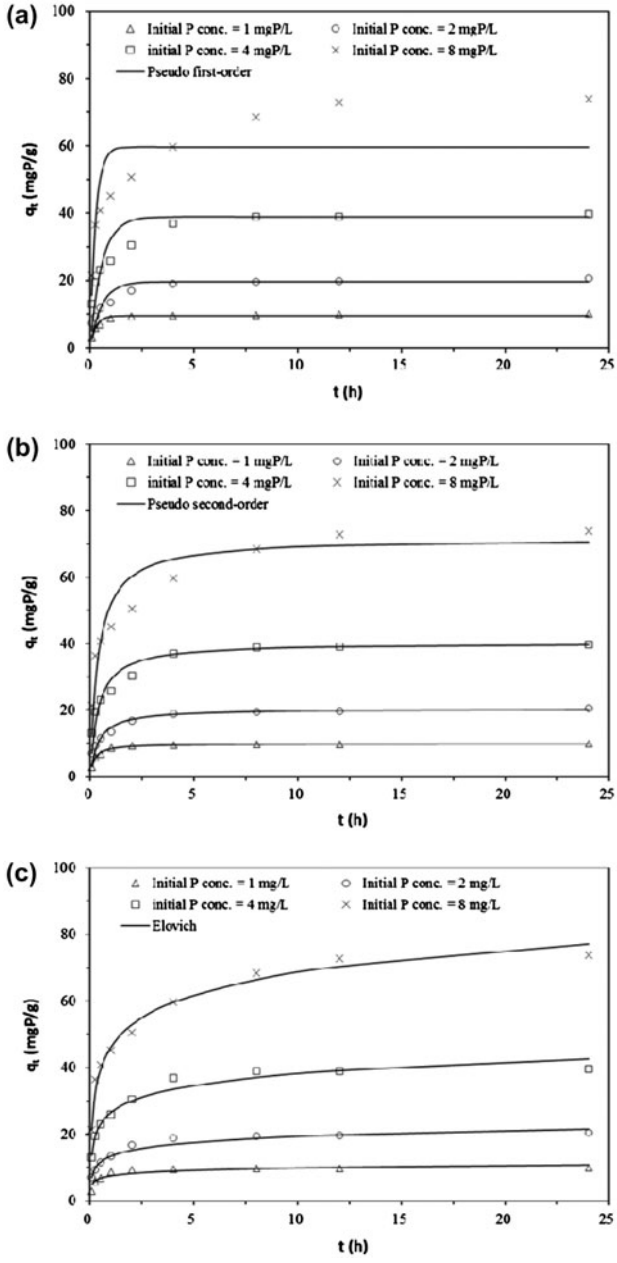

Fig. 3. Kinetic model analyses: (a) pseudo-first-order model, (b) pseudo-second-order model, and (c) Elovich model. Model parameters are presented in Table 1.

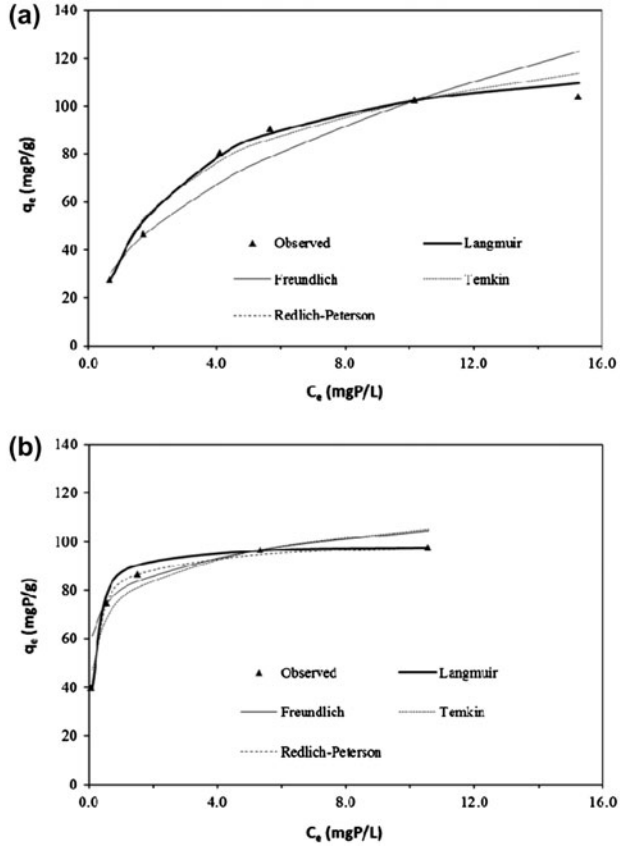

Fig. 4. Equilibrium model analyses: (a) hydrocalumite dose = 0.05 g/L and (b) hydrocalumite dose = 0.1 g/L. Model parameters are presented in Table 2.

reaction time = 24 h) and a synthetic P solution so as to compare the phosphate removal characteristics. Stream water samples were collected from the Seoho stream located in Suwon, Korea. The ionic composition of the stream water was analyzed using an ion chromatograph (Dionex ICS-3000, Thermo Scientific, Waltham, MA, USA), while the chemical oxygen demand (COD_{cr}) was measured according to a standard method [23]. The stream water had the following composition and chemical properties: NaCl = 2.41 mM, $NaHCO_3$ = 0.38 mM, $Ca(HCO_3)_2$ = 0.67 mM, $CaSO_4$ = 0.17 mM, $MgSO_4$ = 0.20 mM, $Mg(NO_3)_2$ = 0.03 mM, KNO_3 = 0.32 mM, K_2HPO_4 = 1.77×10^{-4} mM, COD_{cr} = 4.2 mg/L, pH 6.9, and ionic strength = 613 μS/cm. The stream water was passed through a 0.2 μm filter prior to the experiments in order to remove microorganisms and suspended particles. For the stream water, which had a very low phosphate concentration (0.017 mg P/L), phosphate was added to establish an initial P concentration of 2 mg P/L [24].

2.3. Model analyses

All model parameters were estimated with the solver add-in function in Microsoft Excel 2010; parameter values were determined by nonlinear regression. The determination coefficient (R^2), chi-square coefficient (χ^2), and sum of absolute error (SAE) were utilized to analyze the experimental data and to confirm the model fitting. The expressions for R^2, χ^2, and SAE are as follows:

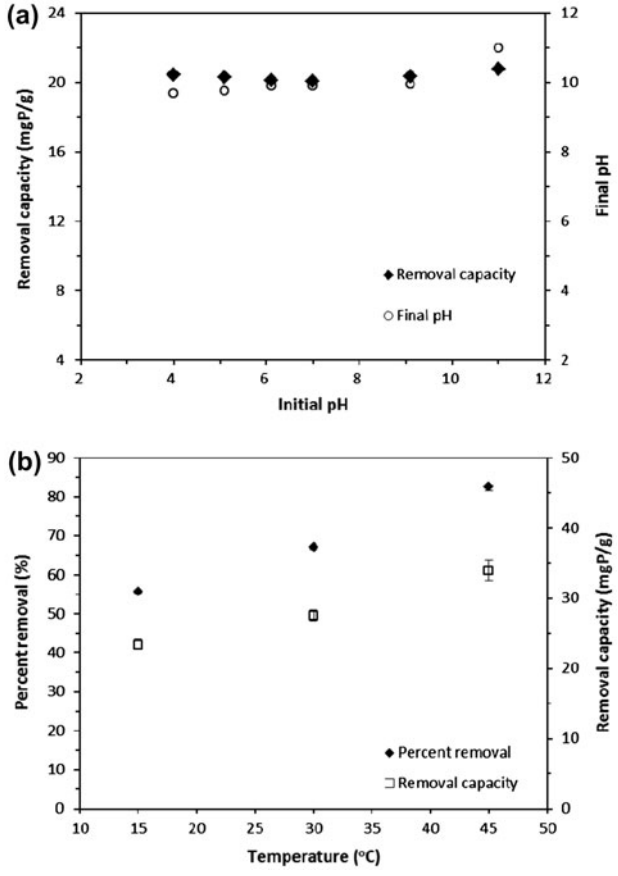

Fig. 5. Phosphate removal by hydrocalumite: (a) effect of initial solution pH and (b) effect of temperature.

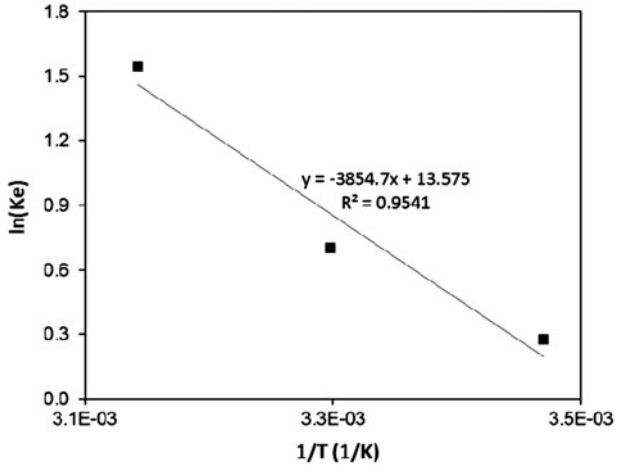

Fig. 6. Thermodynamic model analysis. Model parameters are presented in Table 3.

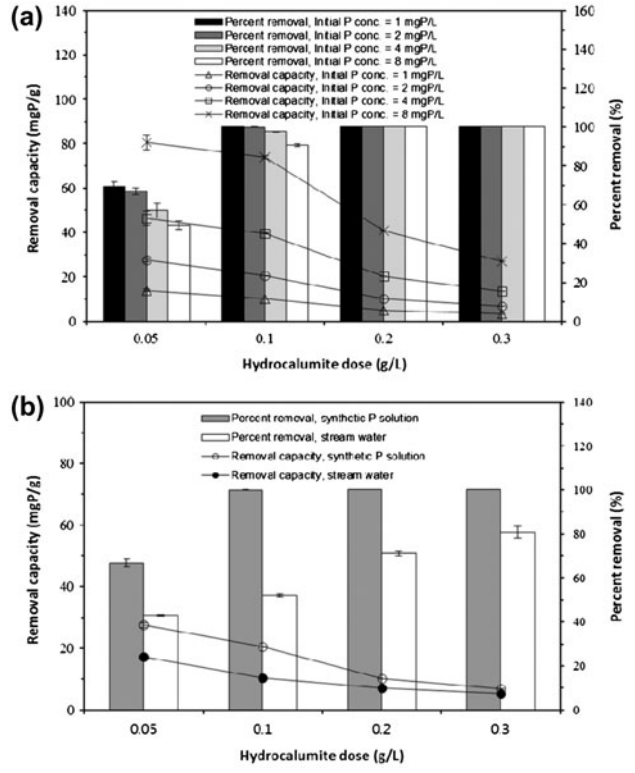

Fig. 7. Phosphate removal by hydrocalumite: (a) effect of hydrocalumite dose and (b) effect of stream water.

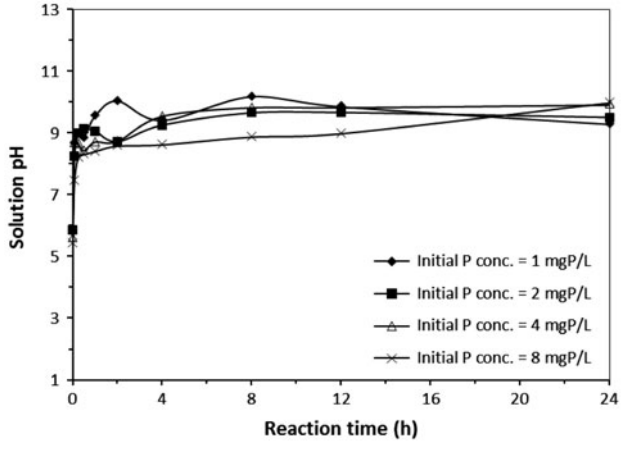

Fig. 8. Changes in solution pH as a function of the reaction time during phosphate removal by hydrocalumite.

$$R^2 = \frac{\sum_{i=1}^{m}(y_c - \bar{y}_e)_i^2}{\sum_{i=1}^{m}(y_c - \bar{y}_e)_i^2 + \sum_{i=1}^{m}(y_c - y_e)_i^2} \quad (1)$$

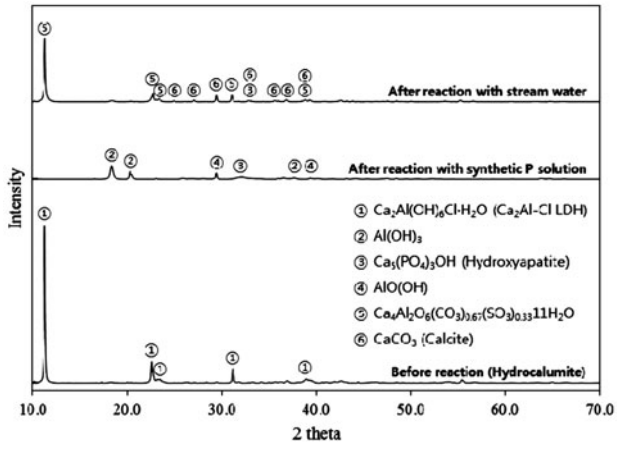

Fig. 9. XRD patterns obtained before and after phosphate removal by hydrocalumite.

$$\chi^2 = \sum_{i=1}^{m}\left[\frac{(y_e - y_c)^2}{y_c}\right]_i \tag{2}$$

$$\mathrm{SAE} = \sum_{i=1}^{n}|y_c - y_e|_i \tag{3}$$

where y_c is the calculated removal capacity from the model, y_e is the measured removal capacity from experiment, and $\bar{y}_e$ is the average of the measured removal capacity.

3. Results and discussion

3.1. Effects of reaction time and initial P concentration

The effect of the reaction time on phosphate removal by hydrocalumite (initial P concentration = 1, 2, 4, and 8 mg P/L; hydrocalumite dose = 0.1 g/L) is shown in Fig. 2(a). At an initial P concentration of 1 mg P/L, the phosphate removal capacity gradually increased, reaching 10.06 mg P/g after a reaction time of 24 h. As the initial P concentration was increased from 2 to 8 mg P/L, the phosphate removal capacity at 24 h increased from 20.58 to 73.86 mg P/g. The experimental data (Fig. 2(a)) were analyzed using pseudo-first-order (Eq. (4)), pseudo-second-order (Eq. (5)), and Elovich (Eq. (6)) kinetic models [25]:

$$q_t = q_e\left(1 - e^{-k_1 t}\right) \tag{4}$$

$$q_t = \frac{k_2 q_e^2 t}{1 + k_2 q_e t} \tag{5}$$

$$q_t = \frac{1}{\beta}\ln(\alpha\beta) + \frac{1}{\beta}\ln t \tag{6}$$

where q_e is the amount of phosphate removed (removal capacity) at equilibrium, q_t is the amount of phosphate removed (removal capacity) at time t, k_1 is the pseudo-first-order rate constant, k_2 is the pseudo-second-order rate constant, α is the initial removal rate constant, and β is the Elovich removal constant.

The results from the kinetic model analyses are presented in Fig. 3, while the kinetic model parameters are provided in Table 1. From the obtained values of R^2, χ^2, and SAE, it was concluded that the Elovich model (Fig. 3(c)) was most suitable for describing the kinetic data, except in the case of a 1 mg P/L concentration (pseudo-second-order model). Parameter values of $\alpha = (4.96 \times 10^2)$–$(1.43 \times 10^3)$ mg P/g/h and $\beta = 0.102$–0.961 g/mg P were determined from the Elovich model (Table 1). The Elovich equation (Eq. (6)) is a rate equation based on the sorption capacity; it is useful for describing chemisorption and understanding the adsorption behavior during the first step of the reaction [25]. Several researchers have employed the Elovich model to describe phosphate removal by various adsorbents, including soils, iron oxides, and lead–zinc tailings [26–29].

The effect of the initial phosphate concentration on phosphate removal by hydrocalumite (hydrocalumite dose = 0.05, 0.1, and 0.2 g/L; reaction time = 24 h) is presented in Fig. 2(b). The percent removal decreased with a rise in the initial P concentration at all hydrocalumite dosages. At a dose of 0.05 g/L, the percent removal decreased from 66.8 to 25.4% with an increase in the initial phosphate concentration from 2 to 20 mg P/L. For a 0.1 g/L dose, the percent removal decreased from 99.9 to 47.8% over the same phosphate concentration range. In the case of a 0.2 g/L dose, the percent removal was 100% at initial P concentrations of 2–10 mg P/L, but decreased slightly to 99.3 and 98.4% at initial P concentrations of 15 and 20 mg P/L, respectively. Meanwhile, the phosphate removal capacity increased with a rise in the initial P concentration at all hydrocalumite dosages. For example, the removal capacity at 0.1 g/L increased from 20.56 to 97.81 mg P/g as the phosphate concentration was increased from 2 to 20 mg P/L. The experimental data in Fig. 2(b) were analyzed with the Langmuir (Eq. (7)), Freundlich (Eq. (8)), Temkin (Eq. (9)), and Redlich–Peterson (Eq. (10)) equilibrium models [30]:

$$q_e = \frac{Q_m K_L C_e}{1 + K_L C_e} \tag{7}$$

Table 1
Kinetic model parameters obtained by fitting models to experimental data

Initial P concentration	1 mg P/L	2 mg P/L	4 mg P/L	8 mg P/L
Pseudo-first-order				
q_e (mg P/g)	9.486	19.604	38.913	59.626
k_1 (1/h)	3.757	1.813	1.789	3.773
R^2	0.952	0.908	0.881	0.683
χ^2	0.346	9.239	17.002	16.036
SAE	3.447	13.779	30.124	73.998
Pseudo-second-order				
q_e (mg P/g)	9.990	20.531	40.288	71.704
k_2 (g/mg P/h)	0.548	0.129	0.066	0.037
R^2	0.993	0.963	0.951	0.907
χ^2	0.042	3.898	6.578	11.790
SAE	1.231	7.228	16.910	45.778
Elovich				
α (mg P/g/h)	1.43×10^3	4.96×10^2	9.48×10^2	1.09×10^3
β (g/mg P)	0.961	0.391	0.197	0.102
R^2	0.851	0.964	0.968	0.985
χ^2	1.201	0.500	0.694	0.923
SAE	6.183	6.056	9.997	16.342

$$q_e = K_F C_e^{\frac{1}{n}} \quad (8)$$

$$q_e = \frac{RT}{b_T} \ln A_T C_e \quad (9)$$

$$q_e = \frac{K_R C_e}{1 + a_R C_e^g} \quad (10)$$

where C_e is the equilibrium concentration of phosphate in the aqueous solution, Q_m is the maximum removal capacity, K_L is the Langmuir constant related to the affinity of the binding sites, K_F is the Freundlich constant associated with the removal capacity, $1/n$ is the Freundlich constant related to the removal intensity, R is the universal gas constant, T is temperature (K), b_T is the Temkin isotherm constant, A_T is the Temkin isotherm equilibrium binding constant (L/g), K_R is the Redlich–Peterson constant related to the removal capacity, a_R is the Redlich–Peterson constant related to the affinity of the binding sites, and g is the Redlich–Peterson constant related to the removal intensity.

The findings from the equilibrium model analyses are presented in Fig. 4, while the corresponding equilibrium model parameters are provided in Table 2. Note that experimental data obtained at a dose of 0.2 g/L were excluded from the model analysis because only two data points were available; at initial P concentrations of 2–10 mg P/L, the percent removal was 100% and thus, equilibrium P concentrations did not exist at these initial P concentrations. The values of R^2, χ^2, and SAE indicated that the Redlich–Peterson model was suitable for describing the equilibrium data. Parameter values of K_R/a_R = 92.53–127.04 mg P/g and g = 0.987–0.999 were determined from the Redlich–Peterson model. The Redlich–Peterson model (Eq. (10)) is an empirical model that combines the Freundlich and Langmuir equations to explain adsorption over a wide range of concentrations. When g is close to unity, the expression reduces to the Langmuir equation [30]. Several researchers have reported that the Redlich–Peterson model is suitable for describing sorption isotherm data [31–33]. From the Langmuir model, the maximum phosphate removal capacity was determined to be 127.53 mg P/g under the given experimental conditions (hydrocalumite dose = 0.05 g/L, initial P concentration = 2–20 mg P/L, reaction time = 24 h). This value was within the range of the phosphate removal capacity of hydrocalumite (69.39–132.57 mg P/g) reported in the literature [2,14,16].

3.2. Effects of pH and temperature

The effect of the initial solution pH on phosphate removal by hydrocalumite (initial P concentration = 2 mg P/L, hydrocalumite dose = 0.1 g/L, reaction time = 24 h) is shown in Fig. 5(a). The phosphate removal capacity remained in the

Table 2
Isotherm parameters obtained by fitting models to experimental data

Hydrocalumite dose	0.05 g/L	0.1 g/L
Langmuir		
Q_m (mg P/g)	127.53	98.84
K_L (L/mg P)	0.403	6.948
R^2	0.987	0.992
χ^2	1.175	0.370
SAE	14.825	8.116
Freundlich		
K_F (L/g)	36.25	79.84
1/n	0.448	0.114
R^2	0.889	0.877
χ^2	7.214	12.235
SAE	46.077	31.210
Temkin		
A_T (L/g)	3.95	469.51
b_T (J/mol)	90.80	204.22
R^2	0.968	0.924
χ^2	2.339	2.763
SAE	24.410	26.268
Redlich–Peterson		
K_R (L/g)	51.68	754.93
a_R (L/mg P)	0.407	8.159
K_R/a_R (mg P/g)	127.04	92.53
g	0.999	0.973
R^2	0.987	0.999
χ^2	1.204	0.043
SAE	14.905	2.354

range of 20.10–20.76 mg P/g even as the initial pH was increased from 4.0 to 11.0, indicating that phosphate removal by hydrocalumite was not sensitive to changes in the pH. Therefore, hydrocalumite could be applied for phosphate removal under various pH conditions. It should be noted that in the initial pH range of 4.0–9.1, the final (equilibrium) pH increased to 9.7–10.0 after the removal experiments. Similar findings were reported by Oladoja et al. [2], who noted that the phosphate removal capacity changed slightly from 98.7 to 99.2 mg/g as the initial pH was increased from 7 to 10. The authors found that the equilibrium pH at the end of the reaction was higher than the initial pH. Ashekuzzaman and Jiang [14] reported that the phosphate removal rates of Ca-based (Ca–Al–NO_3 and Ca–Fe–NO_3) LDHs remained relatively constant (~98%) even though the initial pH was varied from 3.5 to 10.5. The authors also noted that the final pH remained at 10.5 when initial pH values in the range of 3.5–10.5 were employed.

The effect of temperature on phosphate removal by hydrocalumite (initial P concentration = 2 mg P/L, hydrocalumite dose = 0.05 g/L, reaction time = 24 h) is presented in Fig. 5(b). At 15˚C, the phosphate removal capacity was 23.39 mg P/g with a percent removal of 55.6%. When the temperature was raised to 30˚C, the phosphate removal capacity increased to 27.51 mg P/g with an increase in the percent removal to 66.8%. At 45˚C, the phosphate removal capacity further increased to 33.97 mg P/g with the percent removal reaching 82.4%. These results demonstrated that the phosphate removal process was endothermic. The experimental data in Fig. 5(b) were analyzed to determine relevant thermodynamic parameters using the following relationships [34]:

$$\Delta G^\circ = \Delta H^\circ - T\Delta S^\circ \tag{11}$$

$$\Delta G^\circ = -RT \ln K_e \tag{12}$$

$$\ln(K_e) = \frac{\Delta S^\circ}{R} - \frac{\Delta H^\circ}{RT}; \quad K_e = \frac{aq_e}{C_e} \tag{13}$$

where ΔG° is the change in Gibbs free energy, ΔS° is the change in entropy, ΔH° is the change in enthalpy, K_e is the equilibrium constant (dimensionless), and a is the hydrocalumite dose (g/L). Values of $\Delta S^\circ$and ΔH° were determined by plotting $\ln(K_e)$ vs. $1/T$ using Eq. (13), while the value of ΔG° was calculated from Eq. (11). The thermodynamic analysis results are shown in Fig. 6, and thermodynamic parameters are provided in Table 3. The positive value of ΔH° (32.05 kJ/mol) indicates that phosphate removal by hydrocalumite is an endothermic process, while the positive value of ΔS° (112.86 J/K/mol) suggests that the degree of randomness increased at the interface between the solid and solution during the removal process. The negative values of ΔG° (−0.47 to −3.86 kJ/mol) indicate that the phosphate removal process was spontaneous. Our results are in good agreement with the findings of other researchers who examined the endothermic nature of phosphate removal by Mg–Al LDH [24] and Zn–Al LDH [35].

3.3. Effects of hydrocalumite dose and stream water

The effect of the hydrocalumite dose on phosphate removal (initial P concentration = 1–8 mg P/L, hydrocalumite dose = 0.05–0.3 g/L, reaction time = 24 h) is shown in Fig. 7(a). The percent removal increased with a rise in the adsorbent dose from 0.05 to 0.3 g/L. For example, when the initial P concentration was 8 mg P/L, the percent removal was 49.4% at a hydro-

Table 3
Thermodynamic parameters for phosphate removal by hydrocalumite

Temp. (°C)	ΔH° (kJ/mol)	ΔS° (J/K mol)	ΔG° (kJ/mol)
15	32.05	112.86	−0.47
30			−2.17
45			−3.86

calumite dose of 0.05 g/L and 90.7% at a dose of 0.1 g/L. The percent removal reached 100% at 0.2 g/L. A decrease in the removal capacity was observed with an increase in the hydrocalumite dose from 0.05 to 0.3 g/L. When the initial P concentration was 8 mg P/L, the removal capacity was 80.51 mg P/g at 0.05 g/L and 73.86 mg P/g at 0.1 g/L. The removal capacity decreased to 40.74 mg P/g at 0.2 g L, and then decreased further to 27.16 mg P/g at 0.3 g/L.

The phosphate removal characteristics for a synthetic phosphate solution and stream water (initial P concentration = 2 mg P/L, hydrocalumite dose = 0.05–0.3 g/L, reaction time = 24 h) are compared in Fig. 7(b). The removal capacity in the synthetic solution changed from 27.51 to 6.86 mg P/g with a change in the hydrocalumite dose from 0.05 to 0.3 g/L, whereas the percent removal varied from 66.8 to 100% over the same hydrocalumite dosage range. In stream water, the removal capacity changed from 17.25 to 5.40 mg P/g as the hydrocalumite dose was varied from 0.05 to 0.3 g/L, while the percent removal changed from 43.0 to 80.8%. The obtained findings indicate that phosphate removal in the stream water was lower than that in the synthetic P solution. Such results could possibly be due to the presence of carbonate ions (CO_3^{2-}) in the stream water, which could interfere with phosphate removal by hydrocalumite through the precipitation of calcium carbonate ($CaCO_3$, calcite) [36].

It is known that phosphate removal by hydrocalumite (Ca_2Al–Cl-LDH) can occur via a dissolution–reprecipitation process [4,37]. Hydrocalumite could be dissolved during the reaction, and the resulting Ca and Al ions could react with phosphate ions to form Ca- and Al-phosphate precipitates. Brushite ($CaHPO_4{\cdot}2H_2O$) and aluminum phosphate ($AlPO_4$) could be formed at low pH, whereas hydroxyapatite ($Ca_5(PO_4)_3OH$) could be precipitated at high pH [18]. The solution pH values measured in our first set of batch experiments are presented as a function of the reaction time in Fig. 8. Under the given experimental conditions (initial P concentrations = 1–8 mg P/L, hydrocalumite dose = 0.1 g/L), the solution pH was 5.7 ± 0.2 at 0 h, and then increased sharply to 8.2 ± 0.6 within 5 min of the reaction. The solution pH reached 8.9 ± 0.5 after 1 h and remained above 9.0 thereafter. These results indicate that phosphate could be removed in the form of hydroxyapatite. The XRD patterns acquired before and after the phosphate removal reaction are presented in Fig. 9. Before the reaction, the hydrocalumite pattern contained reflection characteristics of a layered structure, with sharp and intense peaks at low 2θ and less intense peaks at high 2θ. After the reaction with a synthetic P solution, peaks from hydroxyapatite, gibbsite ($Al(OH)_3$), and aluminum oxyhydroxide (AlO(OH)) appeared, while reflections from the LDH phase disappeared. However, after the reaction with stream water, the $Ca_4Al_2O_6(CO_3)_{0.67}(SO_3)_{0.33}{\cdot}11H_2O$ LDH phase remained due to the presence of carbonate and sulfate ions in the stream water samples. Reflections from $Ca_5(PO_4)_3OH$ and $CaCO_3$ also appeared after the reaction with stream water.

4. Conclusions

Phosphate removal by hydrocalumite was examined in this study using batch experiments. It was found that the Elovich model was most suitable for describing the kinetic data, whereas the Redlich–Peterson model provided good fits to the equilibrium data. From pH experiments, it was demonstrated that phosphate removal by hydrocalumite was not sensitive to pH changes between 4.0 and 11.0. A thermodynamic analysis showed that phosphate removal by hydrocalumite increased with a rise in temperature from 15 to 45°C, indicating that the removal process was spontaneous and endothermic. Phosphate removal in stream water was lower than that in a synthetic P solution, possibly due to the presence of carbonate ions in the stream water, which resulted in the precipitation of calcium carbonate.

Acknowledgment

This research was supported by a grant from the Korea Institute of Science and Technology (KIST) institutional program (2E25752).

References

[1] M. Zhang, E.J. Reardon, Removal of B, Cr, Mo, and Se from wastewater by incorporation into hydrocalumite and ettringite, Environ. Sci. Technol. 37 (2003) 2947–2952.
[2] N.A. Oladoja, R.O.A. Adelagun, I.A. Ololade, E.T. Anthony, M.O. Alfred, Synthesis of nano-sized hydrocalumite from a Gastropod shell for aqua system

phosphate removal, Sep. Purif. Technol. 124 (2014) 186–194.
[3] P. Zhang, G. Qian, H. Shi, X. Ruan, J. Yang, R.L. Frost, Mechanism of interaction of hydrocalumites (Ca/Al-LDH) with methyl orange and acidic scarlet GR, J. Colloid Interface Sci. 365 (2012) 110–116.
[4] J.Z. Zhou, L. Feng, J. Zhao, J. Liu, Q. Liu, J. Zhang, G. Qian, Efficient and controllable phosphate removal on hydrocalumite by multi-step treatment based on pH-dependent precipitation, Chem. Eng. J. 185–186 (2012) 219–225.
[5] K.H. Goh, T.T. Lim, Z. Dong, Application of layered double hydroxides for removal of oxyanions: A review, Water Res. 42 (2008) 1343–1368.
[6] F. Cavani, F. Trifirò, A. Vaccari, Hydrotalcite-type anionic clays: Preparation, properties and applications, Catal. Today 11 (1991) 173–301.
[7] G.P. Gillman, A simple technology for arsenic removal from drinking water using hydrotalcite, Sci. Total Environ. 366 (2006) 926–931.
[8] R. Liu, R.L. Frost, W.N. Martens, Absorption of the selenite anion from aqueous solutions by thermally activated layered double hydroxide, Water Res. 43 (2009) 1323–1329.
[9] S.J. Palmer, R.L. Frost, Use of hydrotalcites for the removal of toxic anions from aqueous solutions, Ind. Eng. Chem. Res. 49 (2010) 8969–8976.
[10] J.A. Park, C.G. Lee, J.H. Kim, J.K. Kang, I. Lee, S.B. Kim, Removal of bacteriophage MS2 from aqueous solution using Mg–Fe layered double hydroxides, J. Environ. Sci. Health, A 46 (2011) 1683–1689.
[11] J.H. Kim, C.G. Lee, J.A. Park, J.K. Kang, S.Y. Yoon, S.B. Kim, Fluoride removal using calcined Mg/Al layered double hydroxides at high fluoride concentrations, Water Sci. Technol.: Water Supply 13 (2013) 249–256.
[12] D.L. Correll, The role of phosphorus in the eutrophication of receiving waters: A review, J. Environ. Quality 27 (1998) 261–266.
[13] G.K. Morse, S.W. Brett, J.A. Guy, J.N. Lester, Review: Phosphorus removal and recovery technologies, Sci. Total Environ. 212 (1998) 69–81.
[14] S.M. Ashekuzzaman, J.Q. Jiang, Study on the sorption–desorption–regeneration performance of Ca-, Mg- and CaMg-based layered double hydroxides for removing phosphate from water, Chem. Eng. J. 246 (2014) 97–105.
[15] Y. Xu, Y. Dai, J. Zhou, Z.P. Xu, G. Qian, G.Q.M. Lu, Removal efficiency of arsenate and phosphate from aqueous solution using layered double hydroxide materials: Intercalation vs. precipitation, J. Mater. Chem. 20 (2010) 4684–4691.
[16] G. Qian, L. Feng, J.Z. Zhou, Y. Xu, J. Liu, J. Zhang, Z.P. Xu, Solubility product (Ksp)-controlled removal of chromate and phosphate by hydrocalumite, Chem. Eng. J. 181–182(182) (2012) 251–258.
[17] J. Zhao, Y. Dai, Y. Lu, X. Ruan, G. Qian, Y. Xu, Effective phosphate uptake and inhibition on *M. aeruginosa* by Friedel-based adsorbent, Desalin. Water Treat. 52 (2014) 791–796.
[18] Y. Lu, H. Hou, J. Zhao, J. Zhou, J. Liu, L. Feng, G. Qian, Y. Xu, Enhanced removal of phosphate by hydrocalumite: Synergism of $AlPO_4$ and $CaHPO_4{\cdot}2H_2O$ precipitation, Desalin. Water Treat. (2015), doi:10.1080/19443994.2015.1031187.
[19] E. Gombos, K. Barkács, T. Felföldi, C. Vértes, M. Makó, G. Palkó, G. Záray, Removal of organic matters in wastewater treatment by ferrate(VI)-technology, Microchem. J. 107 (2013) 115–120.
[20] C. Li, J. Ma, J. Shen, Removal of phosphate from secondary effluent with Fe^{2+} enhanced by H_2O_2 at nature pH/neutral pH, J. Hazard. Mater. 166 (2009) 891–896.
[21] Y.U. Han, W.S. Lee, C.G. Lee, S.J. Park, K.W. Kim, S.B. Kim, Entrapment of Mg–Al layered double hydroxide in calcium alginate beads for phosphate removal from aqueous solution, Desalin. Water Treat. 36 (2011) 178–186.
[22] APHA (American Public Health Association), Standard Methods for the Examination of Water and Wastewater, APHA, Washington, DC, 1995.
[23] American Public Health Association (APHA), American Water Works Association (AWWA), and Water Pollution Control Federation (WPCF), Standard Methods for the Examination of Water and Wastewater, APHA, Washington, DC, 1981.
[24] J.H. Kim, J.A. Park, J.K. Kang, S.B. Kim, C.G. Lee, S.H. Lee, J.W. Choi, Phosphate sorption to quintinite in aqueous solutions: Kinetic, thermodynamic and equilibrium analyses, Environ. Eng. Res. 20 (2015) 73–78.
[25] S.S. Gupta, K.G. Bhattacharyya, Kinetics of adsorption of metal ions on inorganic materials: A review, Adv. Colloid Interface Sci. 162 (2011) 39–58.
[26] S.H. Chien, W.R. Clayton, application of Elovich equation to the kinetics of phosphate release and sorption in soils, Soil Sci. Soc. Am. J. 44 (1980) 265–268.
[27] H. Kiose, Application of S-shaped $Z(t)$ plots to the kinetics of phosphate sorption by a soil of different phosphorus status, Geoderma 61 (1994) 61–70.
[28] H.D. Ruan, R.J. Gilkes, Kinetics of phosphate sorption and desorption by synthetic aluminous goethite before and after thermal transformation to hematite, Clay Miner. 31 (1996) 63–74.
[29] S. Wang, R. Yuan, X. Yu, C. Mao, Adsorptive removal of phosphate from aqueous solutions using lead-zinc tailings, Water Sci. Technol. 67 (2013) 983–988.
[30] K.Y. Foo, B.H. Hameed, Insights into the modeling of adsorption isotherm systems, Chem. Eng. J. 156 (2010) 2–10.
[31] J.C.Y. Ng, W.H. Cheung, G. McKay, Equilibrium studies for the sorption of lead from effluents using chitosan, Chemosphere 52 (2003) 1021–1030.
[32] K.V. Kumar, K. Porkodi, F. Rocha, Isotherms and thermodynamics by linear and non-linear regression analysis for the sorption of methylene blue onto activated carbon: Comparison of various error functions, J. Hazard. Mater. 151 (2008) 794–804.
[33] Y.S. Ho, Regression analysis for the sorption isotherms of basic dyes on sugarcane dust, Bioresour. Technol. 96 (2005) 1285–1291.
[34] S.Y. Yoon, C.G. Lee, J.A. Park, J.H. Kim, S.B. Kim, S.H. Lee, J.W. Choi, Kinetic, equilibrium and thermodynamic studies for phosphate adsorption to magnetic iron oxide nanoparticles, Chem. Eng. J. 236 (2014) 341–347.

[35] X. Cheng, X. Huang, X. Wang, B. Zhao, A. Chen, D. Sun, Phosphate adsorption from sewage sludge filtrate using zinc–aluminum layered double hydroxides, J. Hazard. Mater. 169 (2009) 958–964.
[36] N. Spanos, P.G. Koutsoukos, Kinetics of precipitation of calcium carbonate in alkaline pH at constant supersaturation. Spontaneous and seeded growth, J. Phys. Chem. B 102 (1998) 6679–6684.
[37] A.V. Radha, P.V. Kamath, C. Shivakumara, Mechanism of the anion exchange reactions of the layered double hydroxides (LDHs) of Ca and Mg with Al, Solid State Sci. 7 (2005) 1180–1187.